The superconducting microcalorimeters array for the X-IFU instrument on board of Athena

Luciano Gottardi

13th Pisa meeting on advanced detectors
Isola d'Elba, Italy, May 24-30, 2015

SRON
Netherlands Institute for Space Research

X-IFU
X-ray Integral Field Unit

Netherlands Organisation for Scientific Research

Advance Telescope for High ENergy Astrophysics

Selected by ESA as the next large mission (L2) to study

The Hot and Energetic Universe

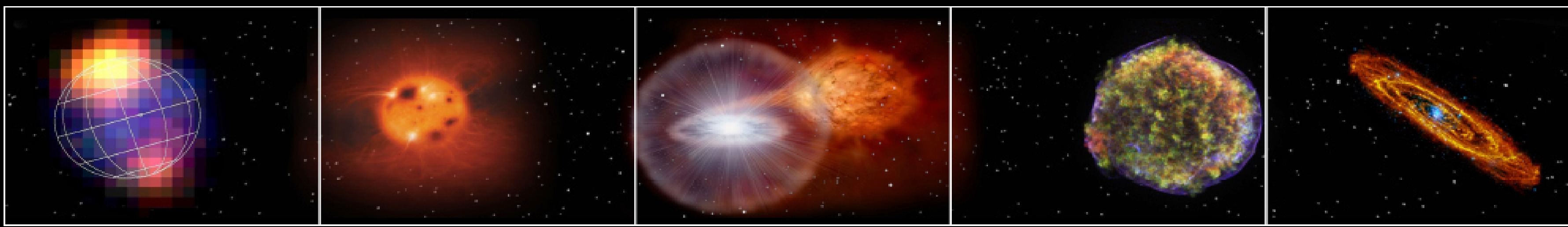

How do black holes grow and influence the Universe?

How does ordinary matter assemble into the large scale structures we see today?

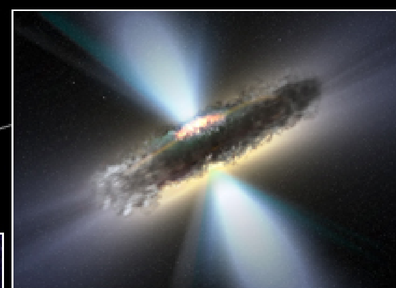

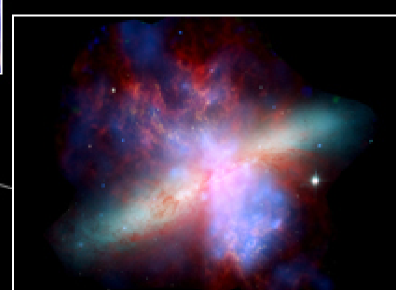

Nandra et al. 2013, 2014

The Athena X-ray Observatory
launch ~2028

Willingale et al, 2013
arXiv1308.6785

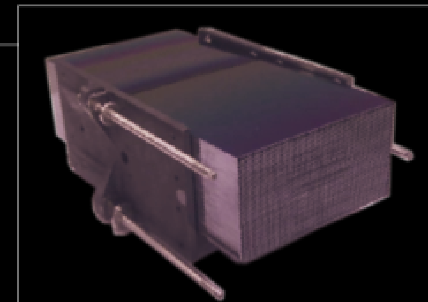

L2 orbit Ariane V
Mass < 5100 kg
Power 2500 W
5 year mission

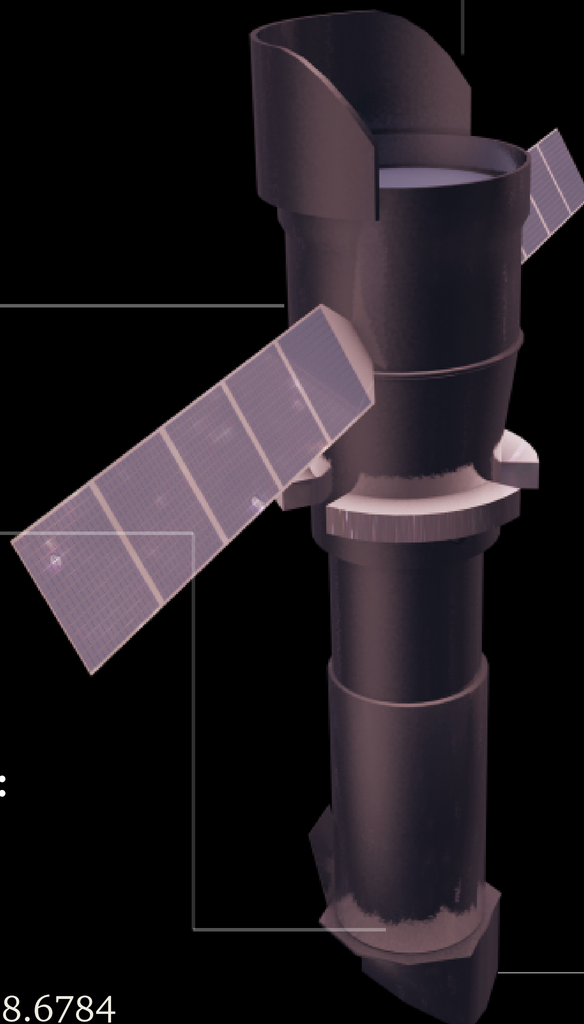

Silicon Pore Optics:
2 m^2 at 1 keV
5 arcsec HEW
Focal length: 12 m
Sensitivity: 3 10^{-17} erg cm^{-2} s^{-1}

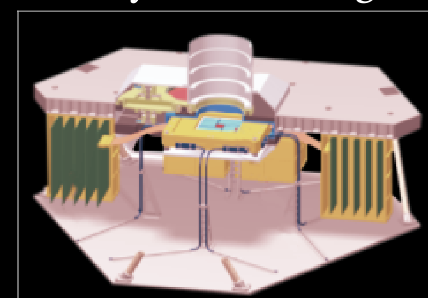

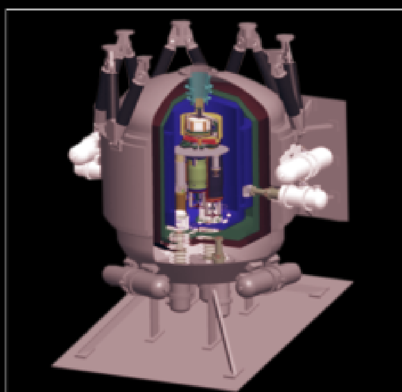

X-ray Integral Field Unit:
dE: 2.5 eV
Field of View: 5 arcmin
Operating temp: 50 mK

Barret et al., 2013 arXiv:1308.6784
L.Ravera et al. SPIE 2014

Wide Field Imager:
dE: 125 eV
Field of View: 40 arcmin
High countrate capability

Rau et al. 2013 arXiv1307.1709

Science with the X-ray Integral Field Unit

spatially resolved high-resolution X-ray spectroscopy

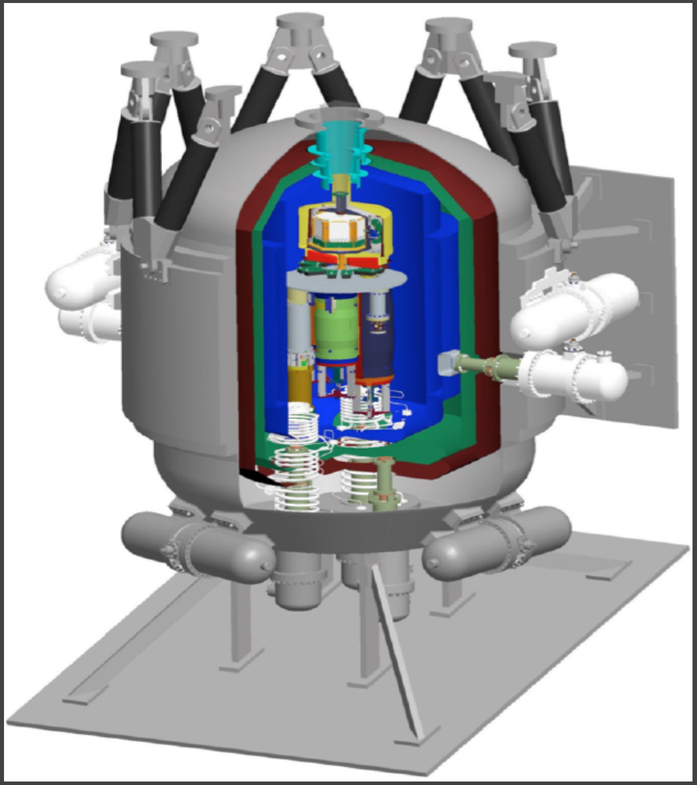

L. Ravera et al., SPIE 2014

the X-IFU must provide breakthrough capabilities for:

- **Mapping in 3D the hot cosmic gas** to measure motions and turbulence: e.g. to study the process of matter assembly in clusters, the AGN feedback on galaxy and cluster scales, …

- **Detecting weak lines** to characterize metals in clusters, the missing baryons in the **W**arm-**H**ot **I**ntergalactic **M**edium, …

The X-IFU instrument on ATHENA

spatially resolved high-resolution X-ray spectroscopy

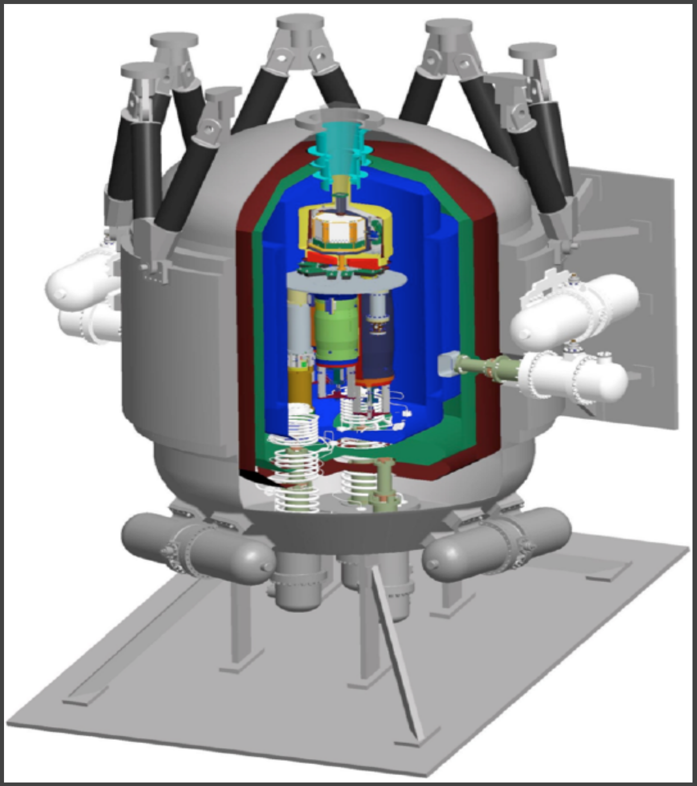

R. den Hartog et al., SPIE (2014)

Energy range:	0.2 -12keV
Energy resolution:	2.5eV (E<7keV)
Field of view:	5 arcmin
Pixel size:	< 5x5 arcsec^2
Non X-ray backgrnd:	< 5x10^{-3} cts/cm^2/keV

These requirements can be met by

• a large array of **3840** Transition Edge Sensors with absorbers of **250 μm x 250 μm** actively shielded
• Multiplexing factor: ~**40 pixels/channel**
• SQUID-based Frequency Domain Multiplexing
• TES based anti-coincidence detector

Bath temperature: **50mK**

SRON X-IFU

Superconducting Transition Edge Sensors

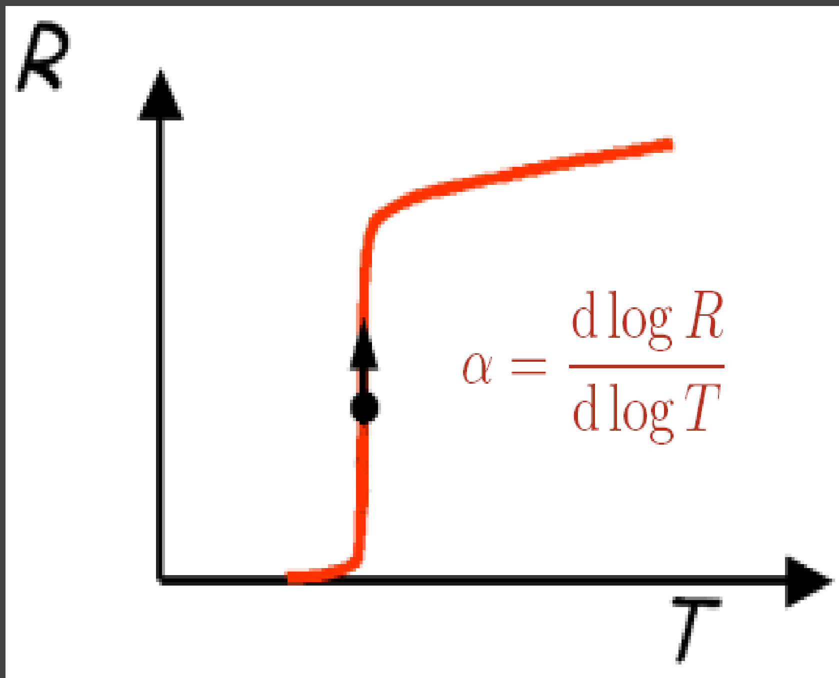

Thin film superconducting bilayer:

Ti/Au
Mo/Au
Mo/Cu

Electrical circuit **Thermal circuit**

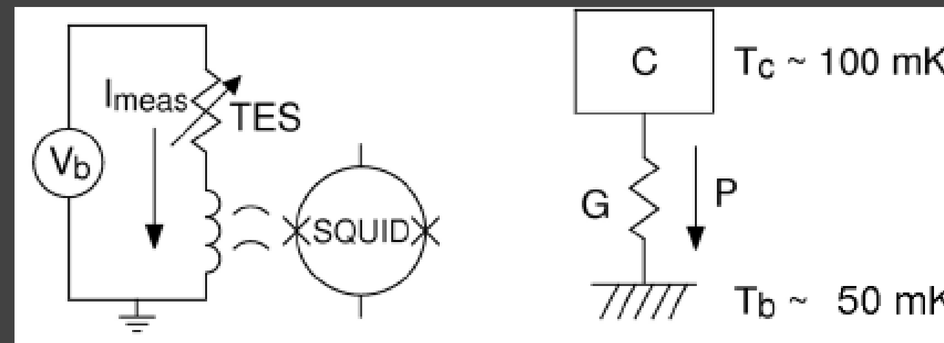

- **Electro-thermal feedback**
- Heat input from photons:
  - → TES temperature and resistance **up**
  - → Joule power **down**
  - → fast recovery
- self biasing in the transition

K. D. Irwin, Appl. Phys. Lett. 66, 1945 (1995)

TES micro-calorimeters

Single photon detector

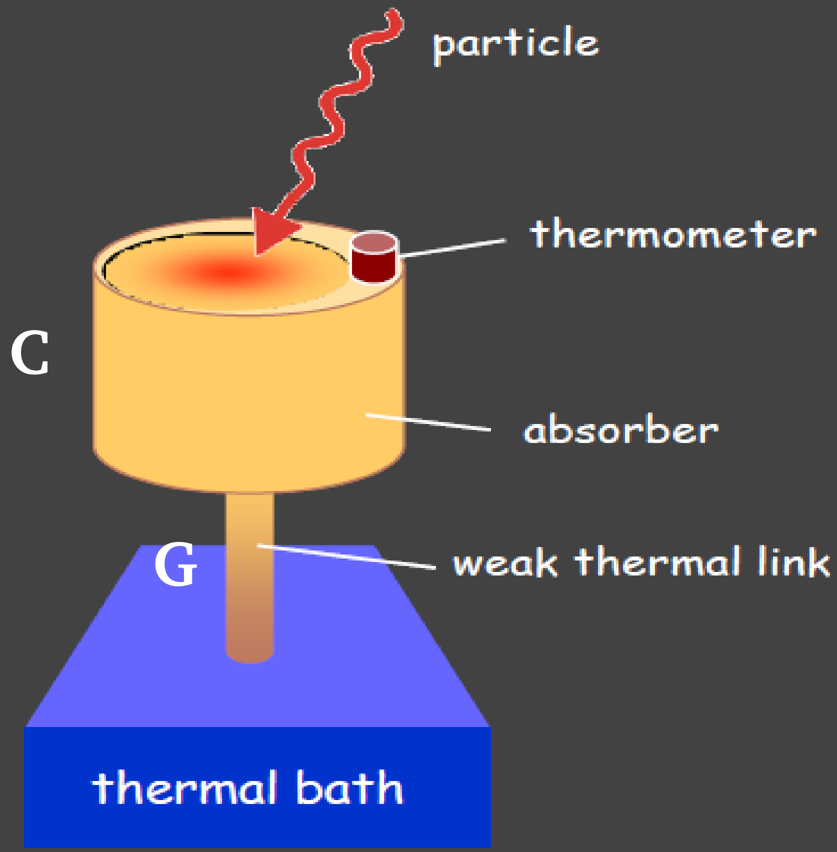

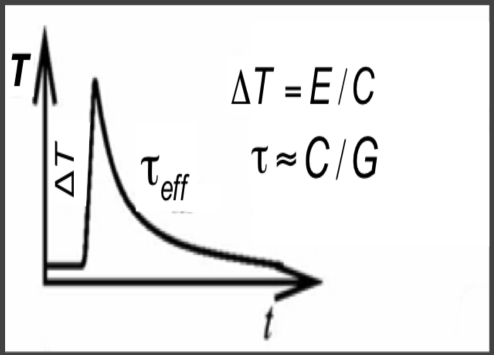

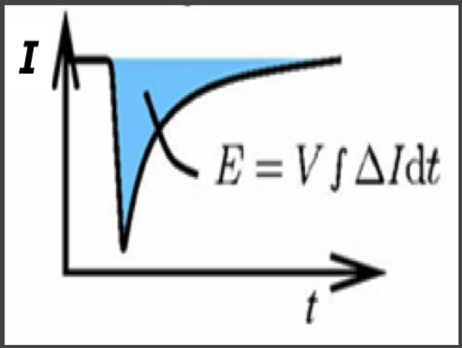

Energy resolution:

$$E_{FWHM} \sim 2.355\sqrt{\frac{4 k_B T_c^2 C}{\alpha}}$$

- Low temperature detector Tc~100mK
- Sharp transition $\alpha \sim 10\text{-}500$
- Small pixels, low C absorbers
- Limited dynamic range: $E_{lin} \propto C/\alpha$

TES micro-calorimeters

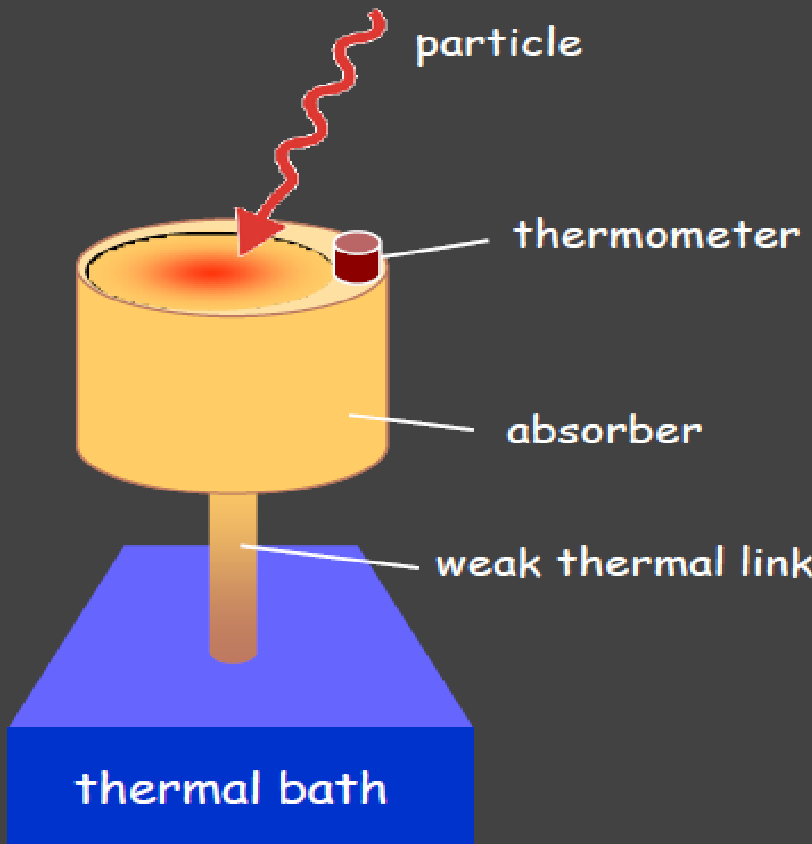

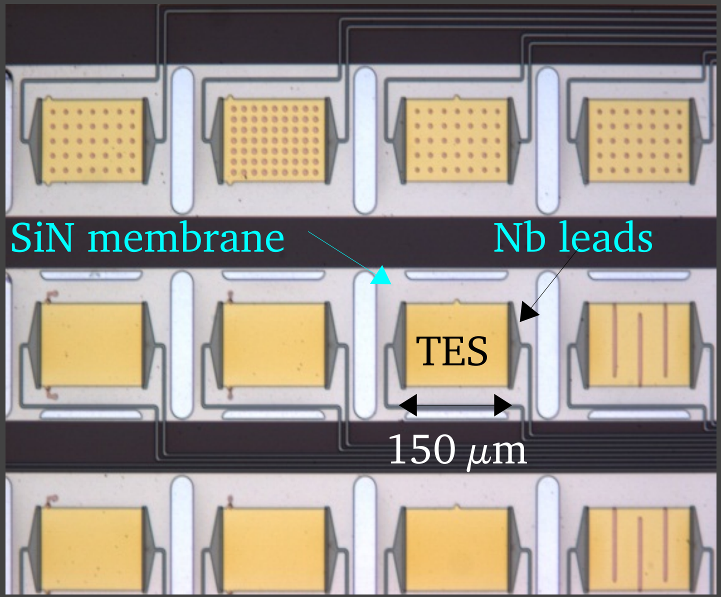

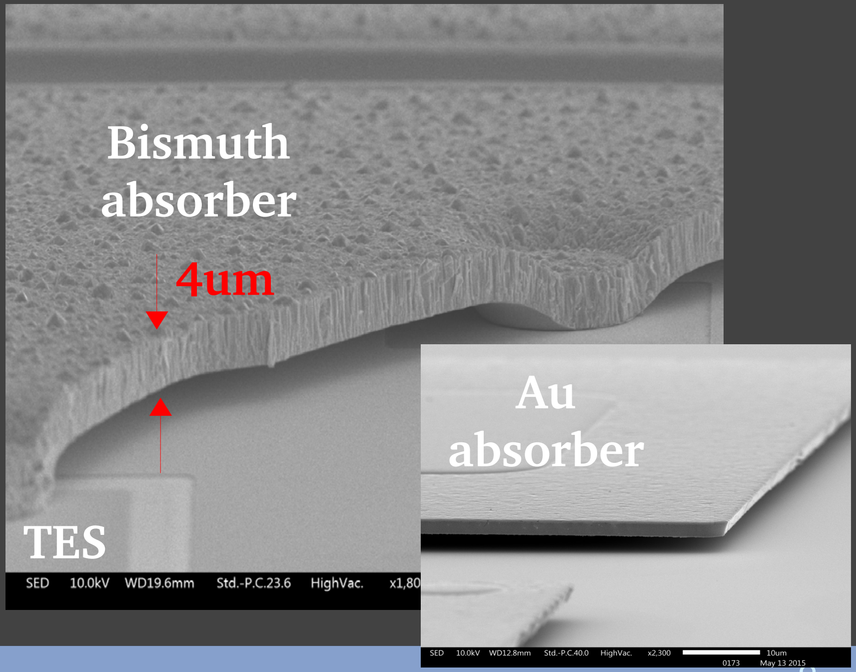

Thin film absorber: Au, Bi,…

TES physics on recently understood

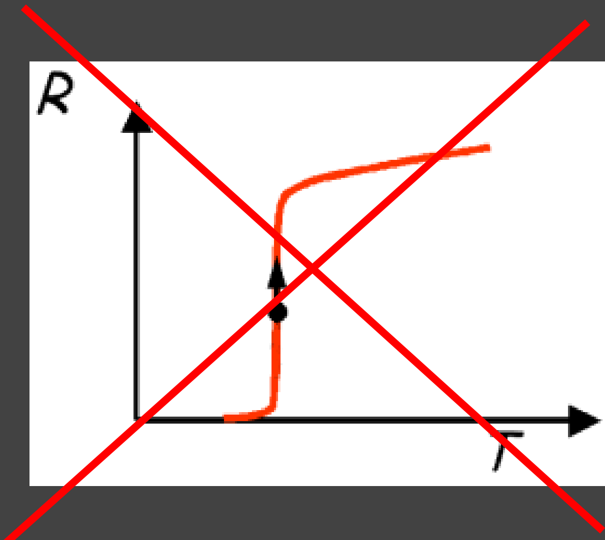

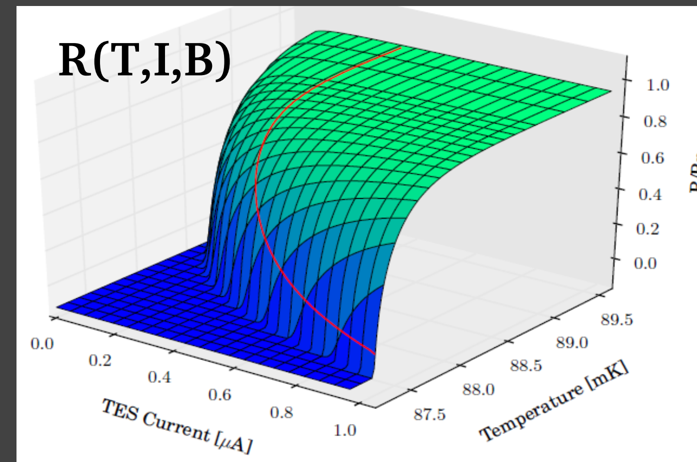

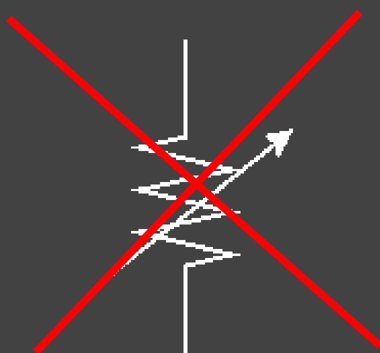

$J_J = J_o \sin \varphi$

$L_J = L_{J\,o} \cos^{-1} \varphi$

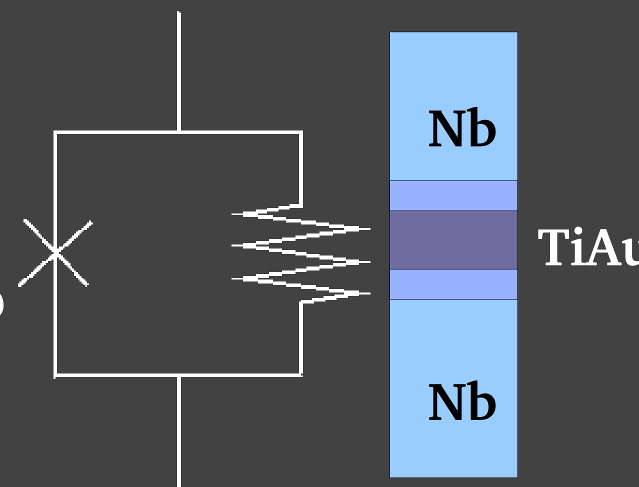

- TES resistance in transition depends on T, I, and B
- TES behaves as a **weak-link (Josephson junction)** due to proximity effect induced by the superconducting Nb leads

Superconducting weak-link effects in TESs

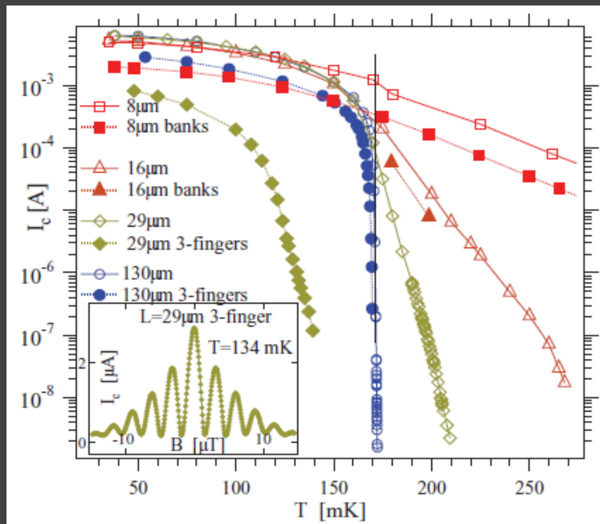

J.Sadleir *et al.* PRL 104, 047003 (2010)
S.Smith *et al.* JAP,114, 074153 (2013)

- Weak-link effects observed at NASA-GSFC with TES microcalorimeters under dc bias

- TES bolometers at SRON under ac-bias: Direct measurement of the Josephson current and of the TES **non-linear inductance**

- Modelling of the resistive transition in a TES using Josephson junction theory

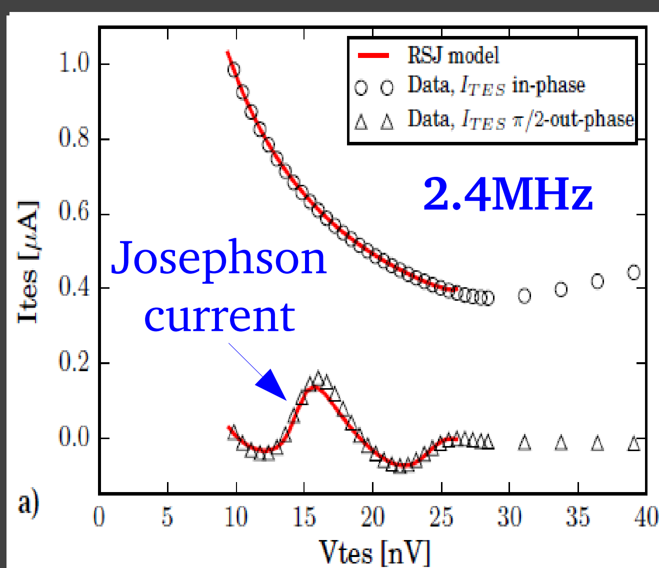

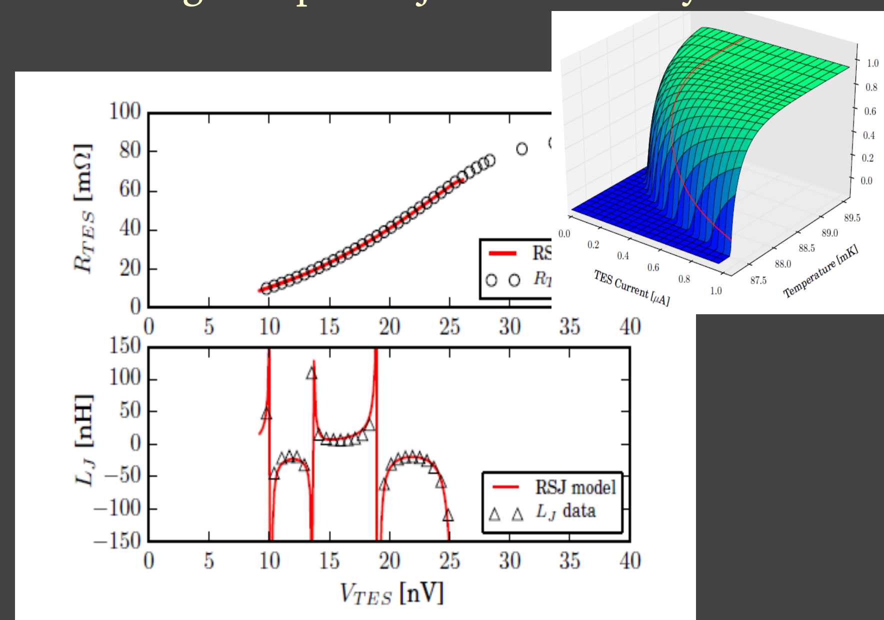

L. Gottardi *et al.* APL, 105, (2014)

TESs are very sensitive detectors

FWHM=1.81 eV@ 6keV
dE_{fwhm}=0.03%

Due to publication right issues this picture has been removed intentionally.
Please contact the author for more info.

courtesy S.Bandler NASA-GSFC

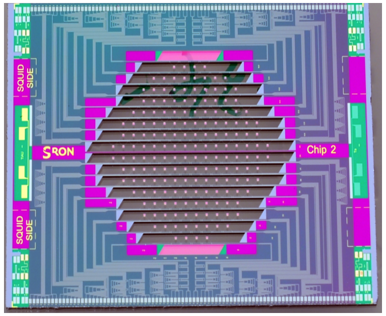

1.3×10^{-19} W/Hz$^{1/2}$

Due to publication right issues this picture has been removed intentionally.
Please contact the author for more info.

T.Suzuki SRON 2015

Current state-of the art of
TES **microcalorimeters**

NASA-Goddard

Current state-of the art of
TES **bolometers**

SRON (SAFARI)

SAFARI

TES bolometers array developed at SRON

for infrared missions

SAFARI

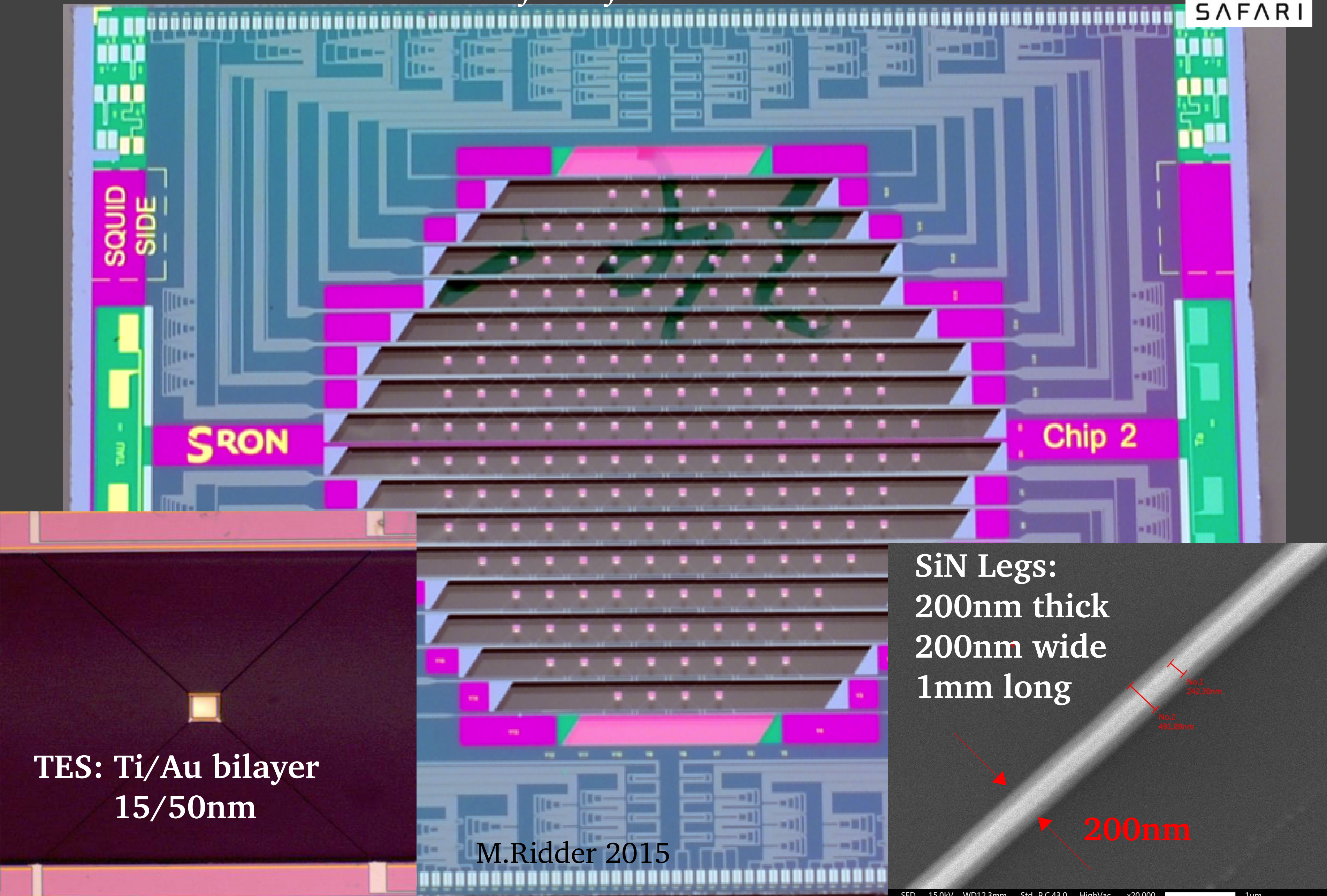

Best performing X-ray microcalorimeters at SRON

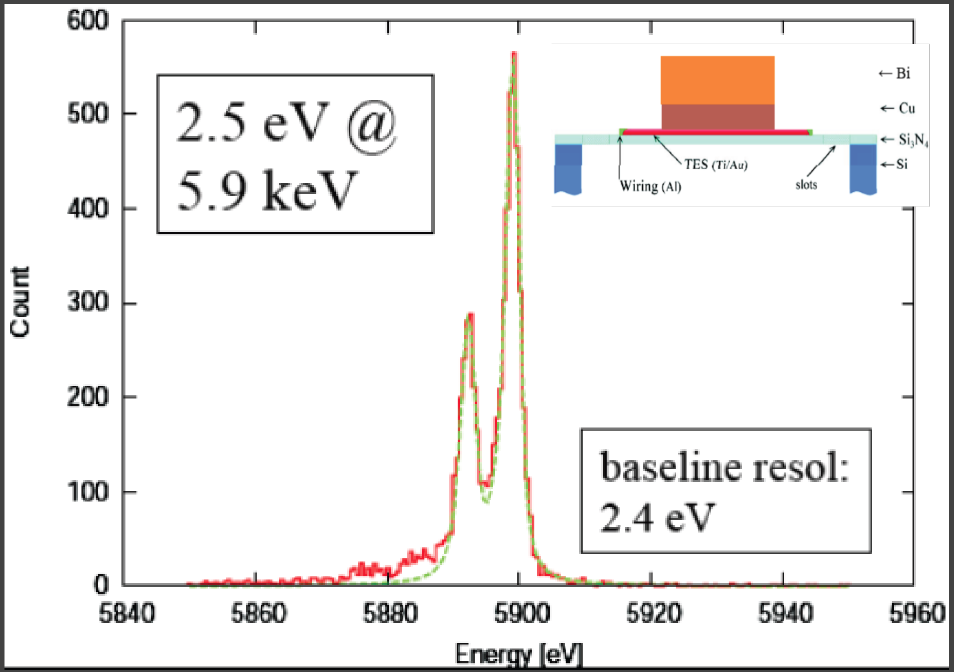

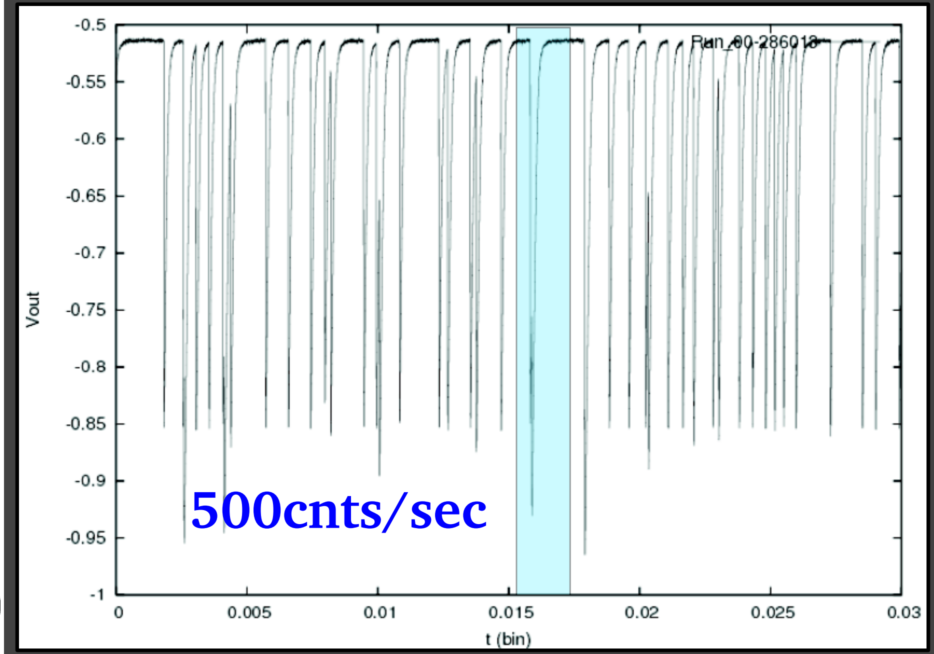

TES: TiAu
thickness: 20/55 nm
size: 150×186 μm2

absorber: Cu/Bi
thickness: 1/2.64 μm
size: 100×100 μm2

- Measurement done under DC bias.
- Stopping power 74%, low filling factor
- Energy scan performed at the Synchrotron Radiation facility BESSY (Berlin)

SRON X-IFU

Best performing X-ray microcalorimeters at SRON

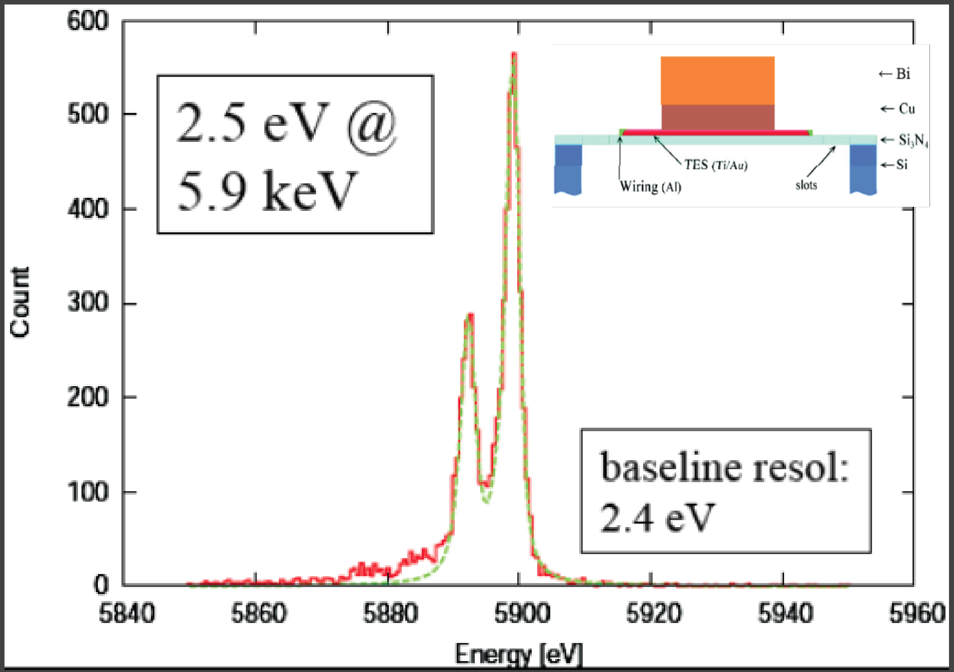

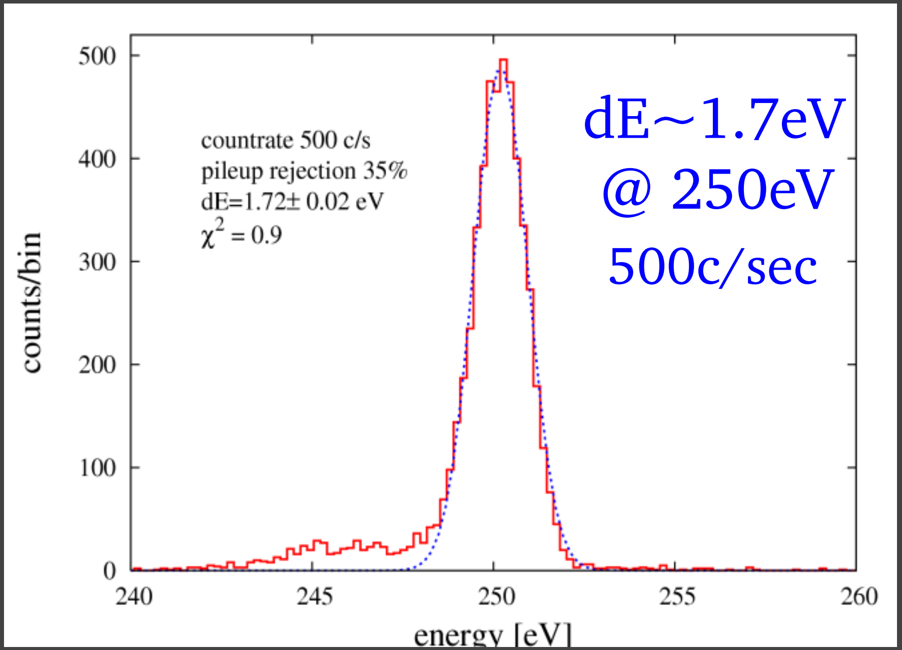

TES: TiAu
thickness: 20/55 nm
size: 150×186 μm2

absorber: Cu/Bi
thickness: 1/2.64 μm
size: 100×100 μm2

- Measurement done under DC bias.
- Stopping power 74%, low filling factor
- Energy scan performed at the Synchrotron Radiation facility BESSY (Berlin)

SRON X-IFU

SRON X-ray TES microcalorimeters array

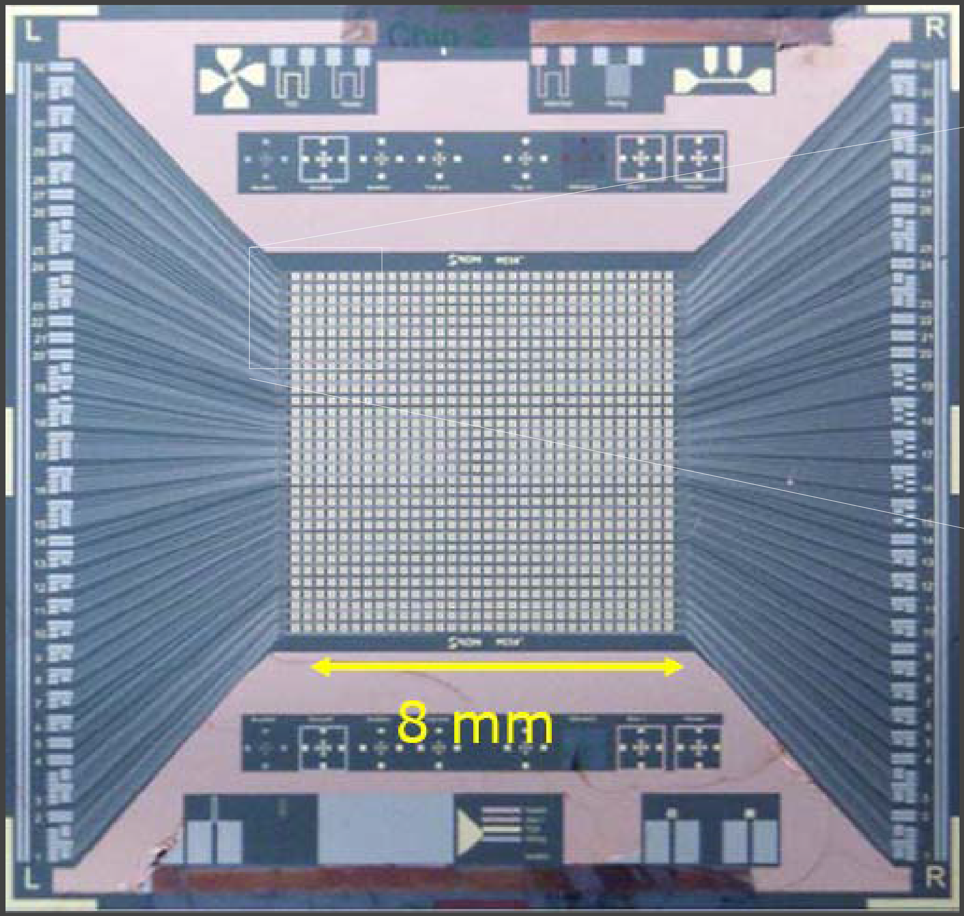

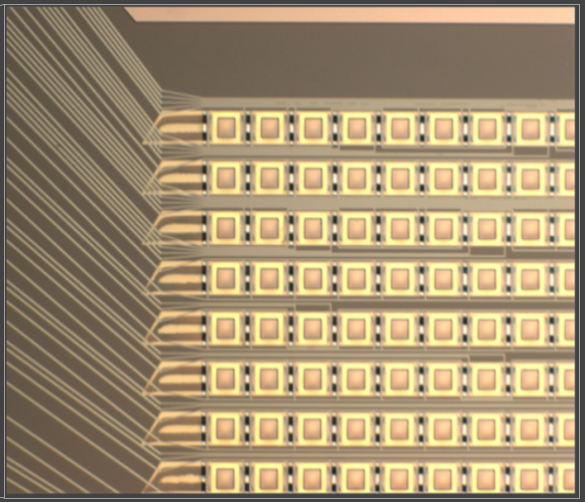

- 32x32 pixels array demonstrator (2006)
- Fully wired from the TESs, only a selection of pixels wired to the chip edge

SRON X-IFU

Detectors array configuration for X-IFU

(Under study)

GODDARD SPACE FLIGHT CENTER

Due to publication right issues this picture has been removed intentionally.
Please contact the author for more info.

QE=94%

courtesy S.Bandler, 2015

Frequency Domain Multiplexing

Multiplexing needed due to limited cooling power and to reduce harness complexity

- **Modulation**: shift in frequency space by multiplication with carrier
- TES works as Amplitude Modulator (AM)
- High Q-factor superconducting LC resonators needed for voltage bias
- Baseband feedback to increase linear dynamic range

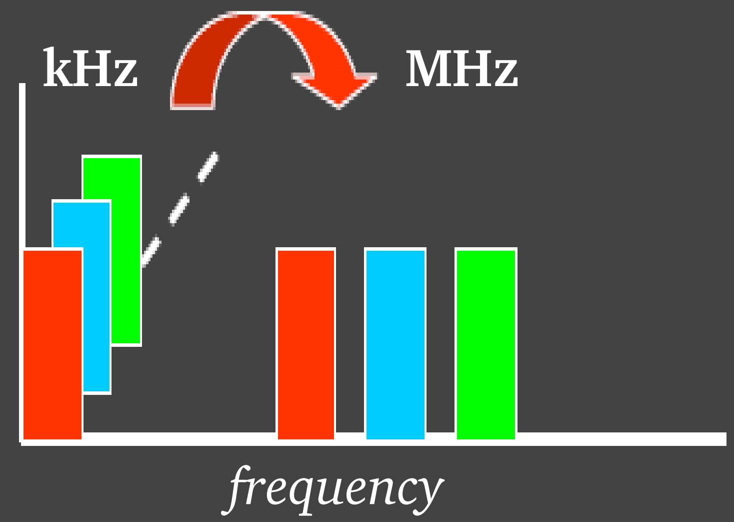

FDM feature

- One TES per row
- One LC filter per TES
- One SQUID amplifier per column
- Voltage bias comb per column

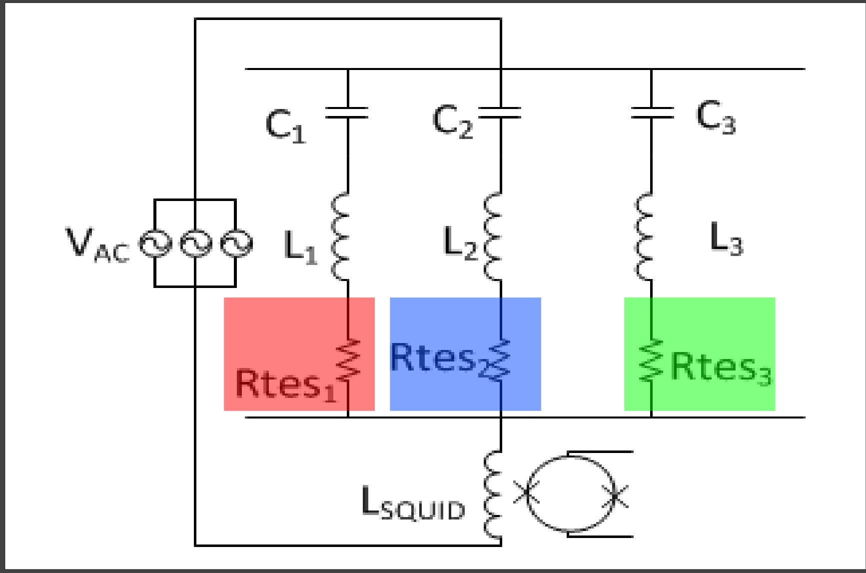

SRON X-IFU

8+ pixels FDM demonstration

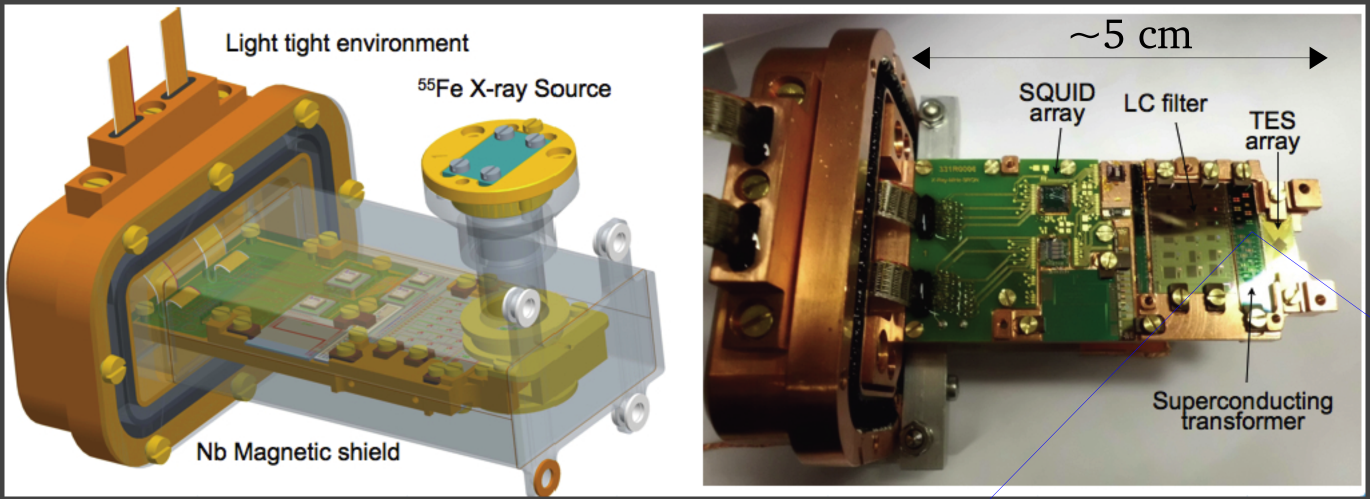

Cryogen-free DR
Leiden Cryogenics

FDM channels

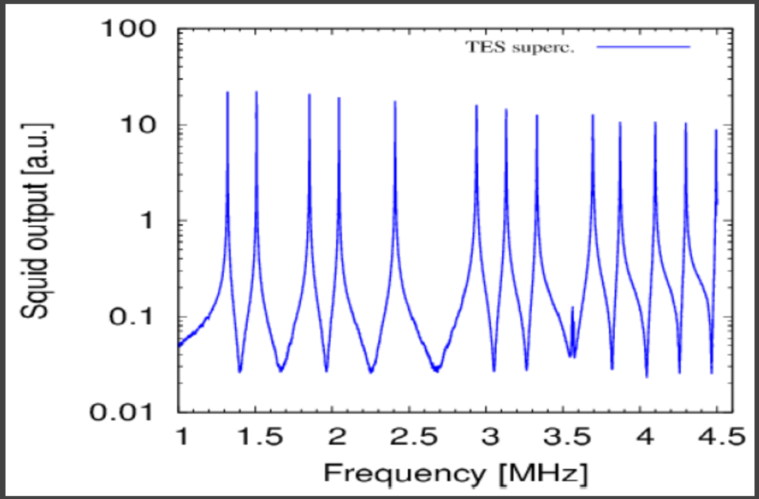

Pixels array from NASA-Goddard

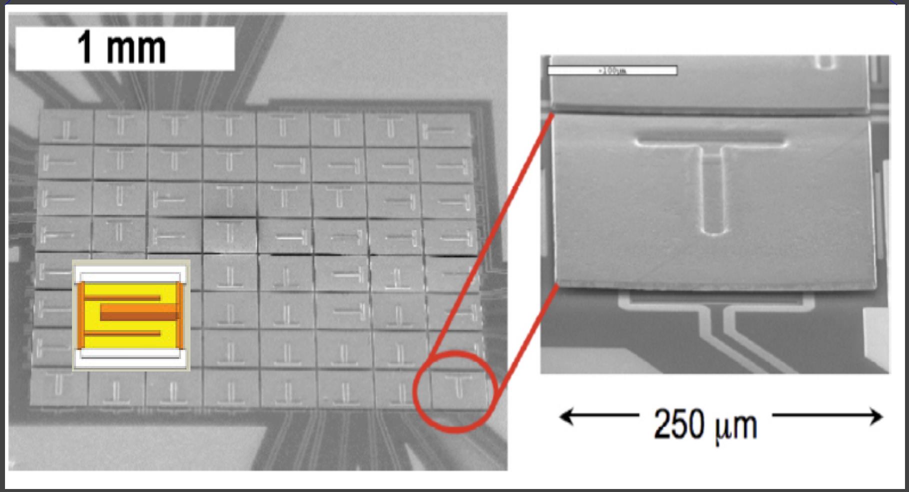

GODDARD SPACE FLIGHT CENTER

SRON X-IFU

Current status FDM demonstration

Almost quantum limited two-stage SQUID amplifier

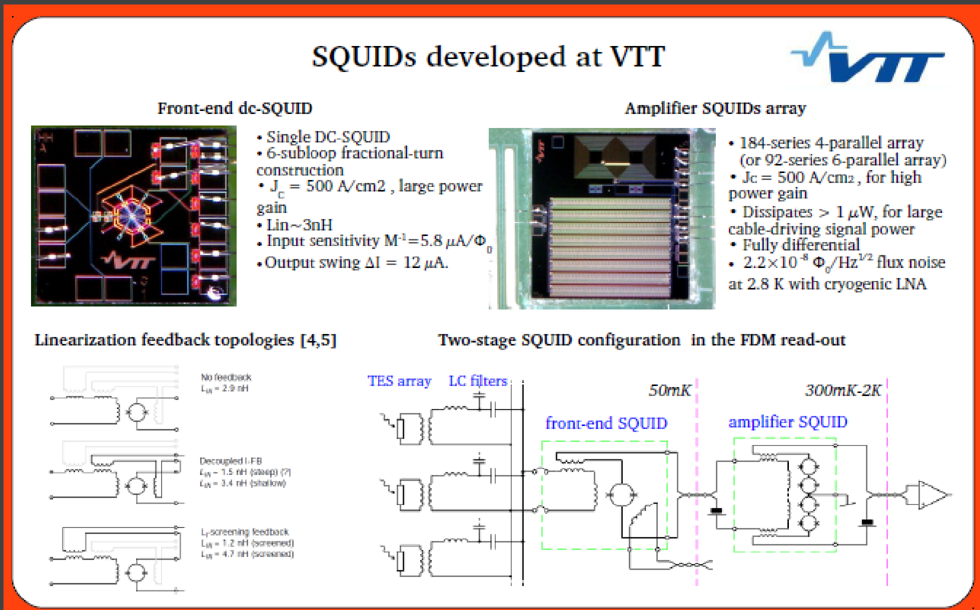

SQUID performance with open-input (a)

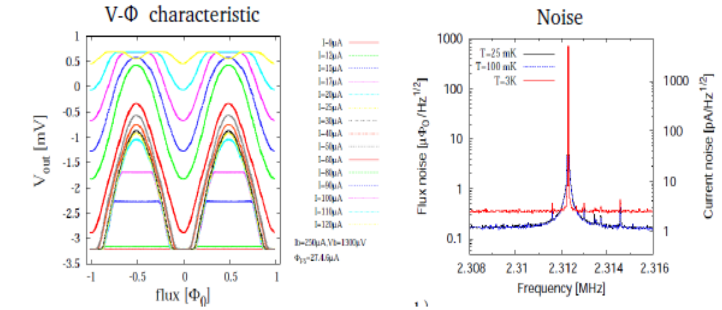

- Flux noise: $S_\Phi^{1/2}=3.5\cdot10^{-7}\ \Phi_0/Hz^{1/2}$ at 3K
  $S_\Phi^{1/2}=1.8\cdot10^{-7}\ \Phi_0/Hz^{1/2}$ at <100mK
- Best energy resolution:

$$\varepsilon=S_\Phi/2L_{SQ} \simeq 9\,\hbar \quad \textit{intrinsic} \quad (L_{SQ}=70\ pH)$$

$$\varepsilon_C=1/2L_{IN}I^2_{NS} \simeq 15\,\hbar \quad \textit{coupled} \quad (L_{IN}=3\ nH)$$

L.Gottardi et al. ASC 2014

Very good SQUID performance with GSFC detectors

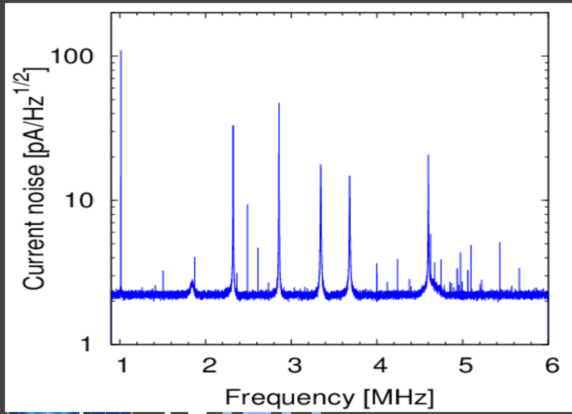

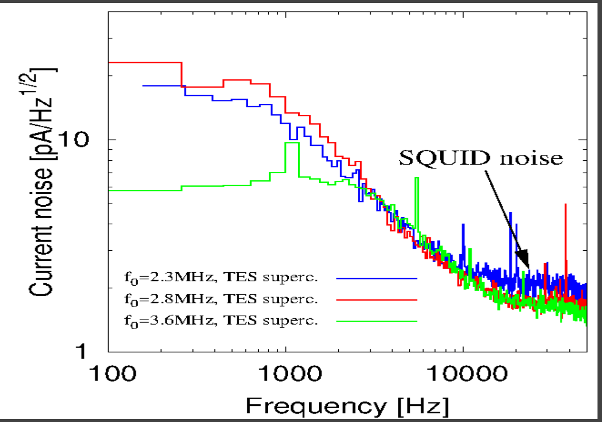

Current status FDM demonstration

2.3MHz
dE~ 2.6±0.1 eV

Due to publication right issues this picture has been removed intentionally.
Please contact the author for more info.

3.7MHz
dE~ 2.7±0.1 eV

Due to publication right issues this picture has been removed intentionally.
Please contact the author for more info.

H. Akamatsu, 2015

- Single pixel high energy resolution demonstrated in the representative frequency range
- Work on-going to improve statistics and the multiplexing performance

Demonstration Model: 4x40 pixels FDM demonstration

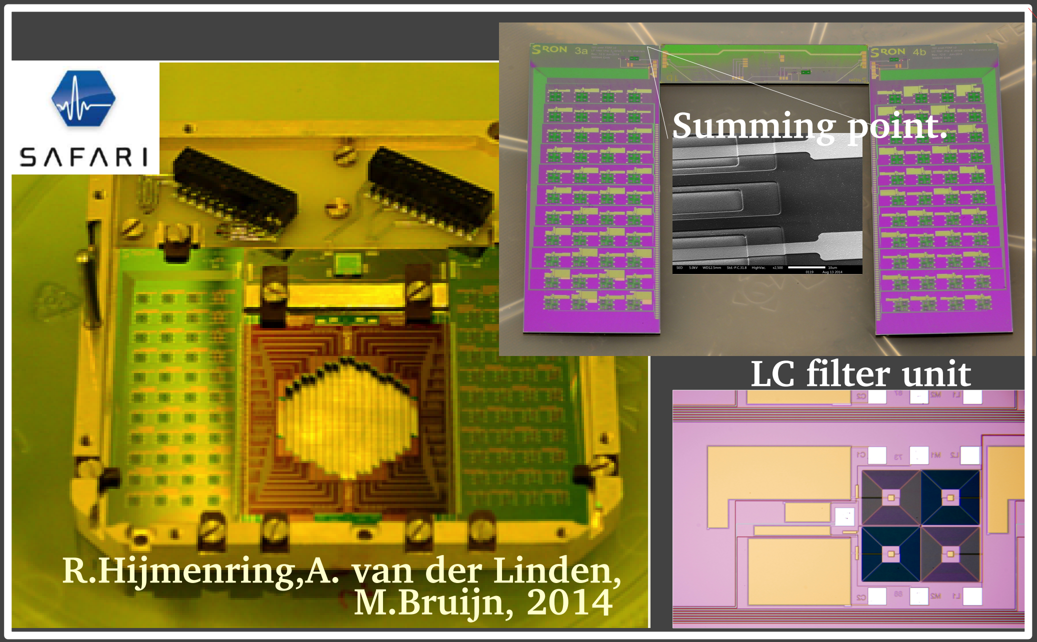

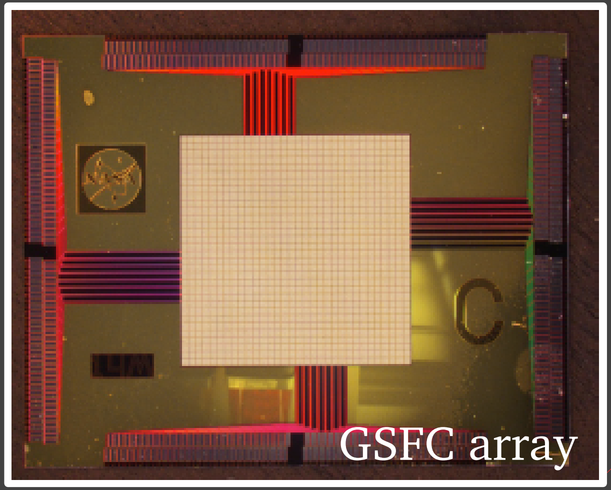

Baseline FPA configuration:
Apply same shield / suspension geometry in DM + EM,
optimize 50 mK geometry for EM

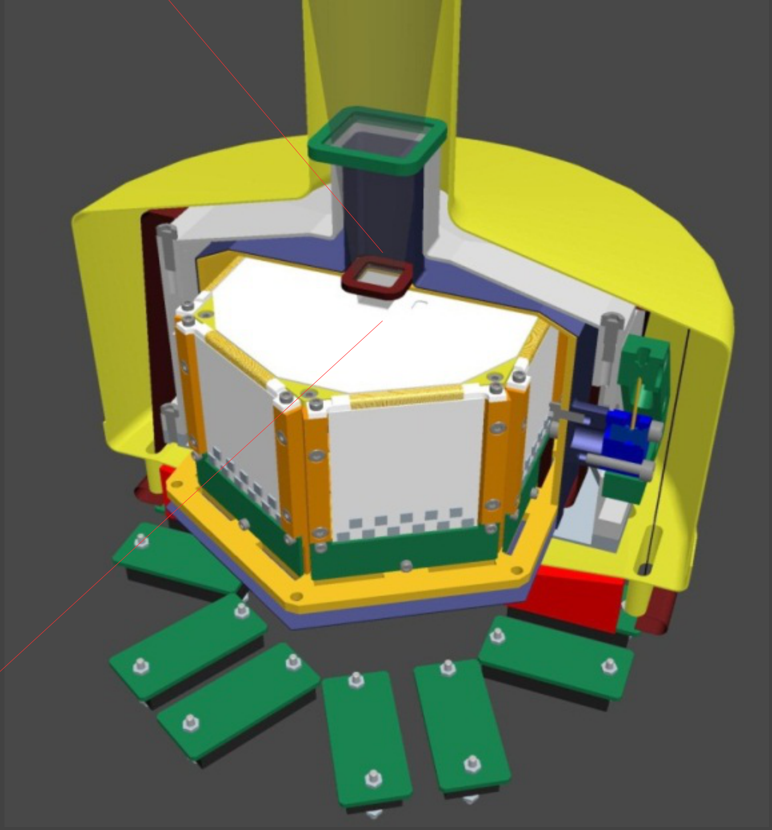

H.van Weers, 2014

Anti coincidence detector

CryoAC 2x2 array design and mechanical I/F with the TES array

Possible integration between the CyroAC and the TES array

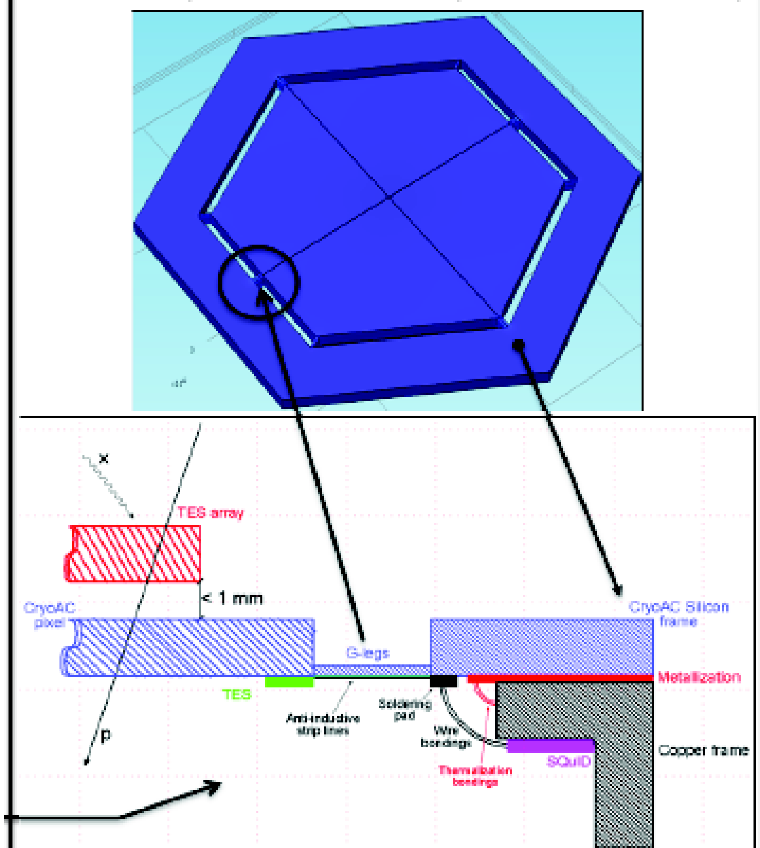

Some measurements from AC-S5

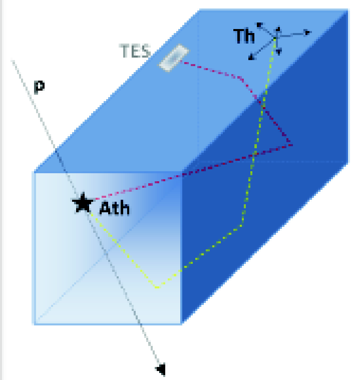

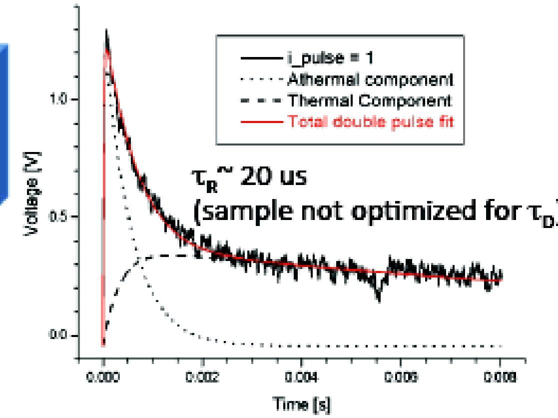

$$E_{measured} = \left(\frac{L}{L+1}\right) \cdot E_d = \left(\frac{L}{L+1}\right) \cdot \varepsilon_{ph \to TES} \cdot E_\gamma$$

AC-S5 illuminated by 60 keV ^{241}Am

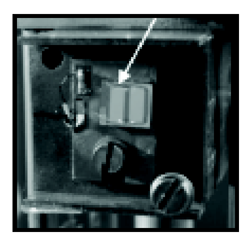

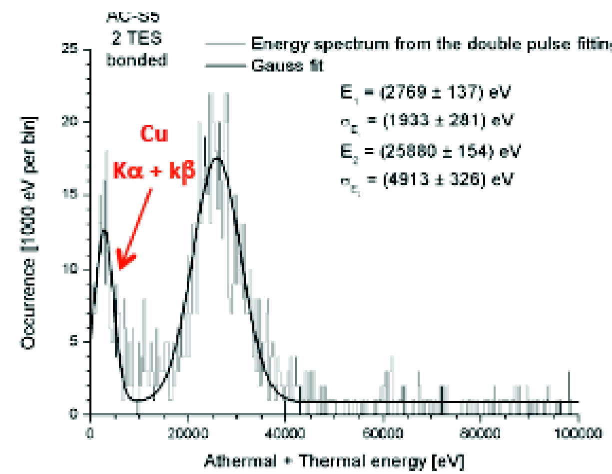

courtesy C. Macculi INAF

Focal plane assembly

FPA technology developments 2011-now:

- Interconnects
- Detector mounting
- Kevlar thermal insulating suspension
- Magnetic shielding:
    - Niobium (superconducting)
    - Cryoperm 10

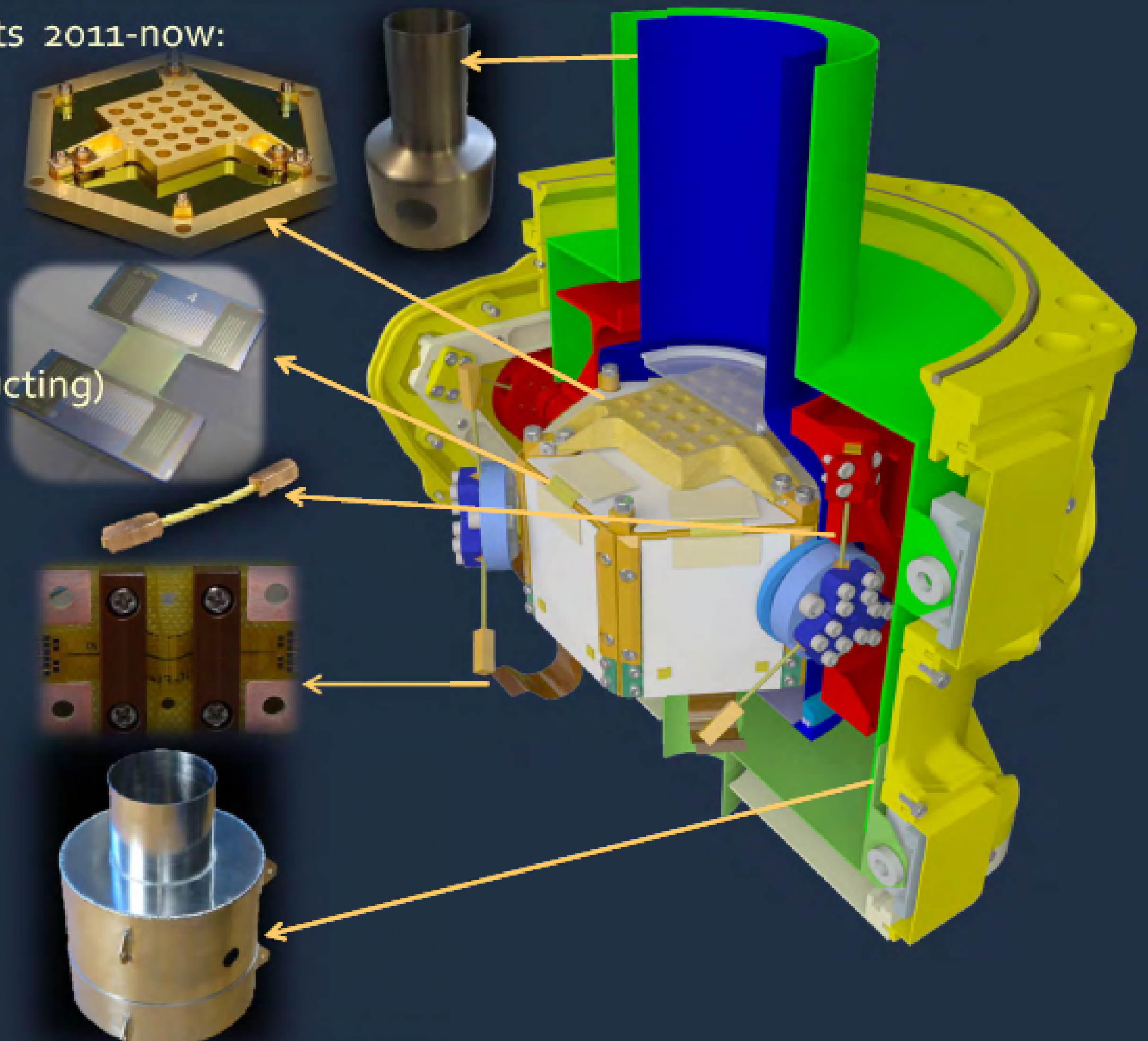

H.van Weers, 2015

Key technology under development at SRON

High Q-factor superconducting LC filters

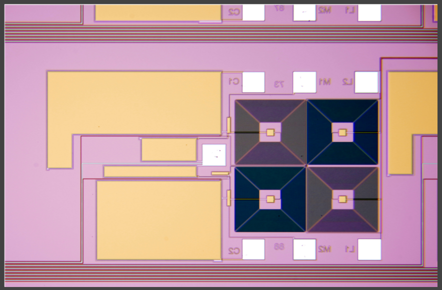

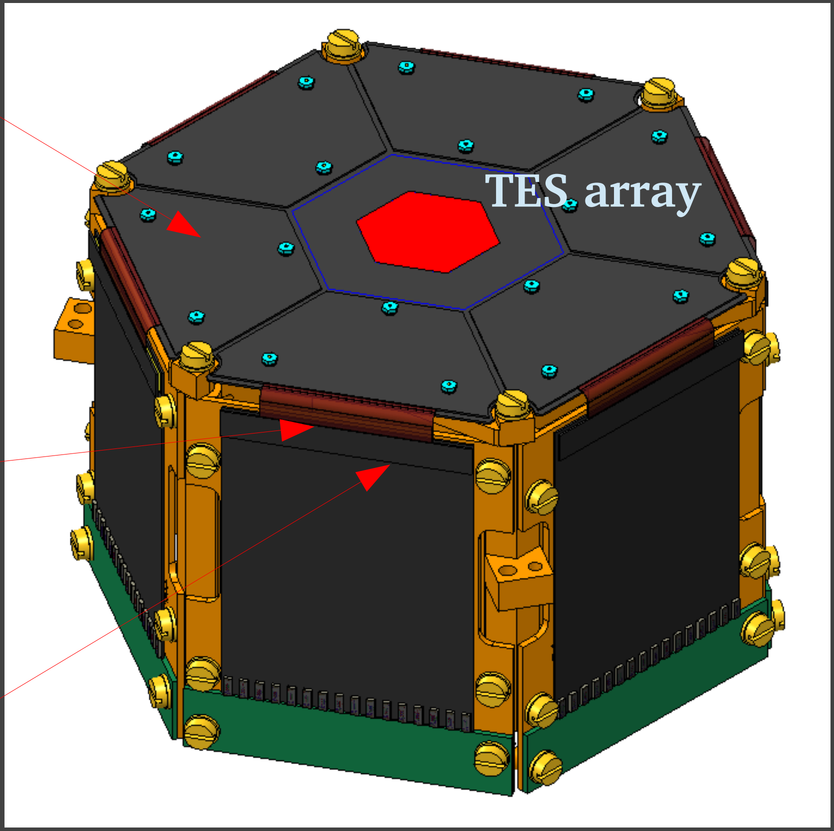

Polyimide flex chips

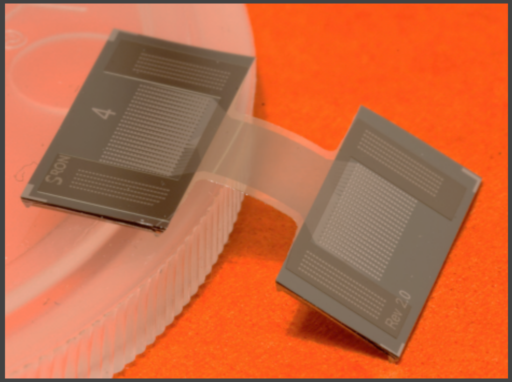

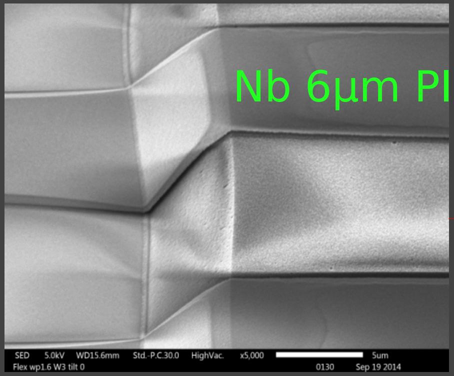

Electroplated Au bumping

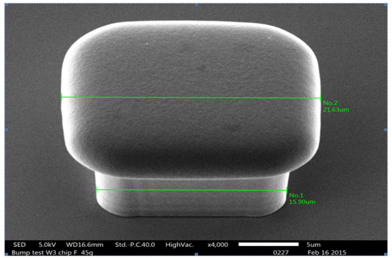

Fig. 10. Typical Au-bump shape (45 degree view) from 15x15 µm photoresist stencil.

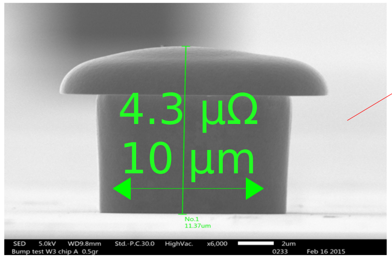

Fig. 11 Typical Au-bump shape (90 degrees side view) from 10x10 µm resist stencil.

Detector cold head

M.Bruijn, 2015

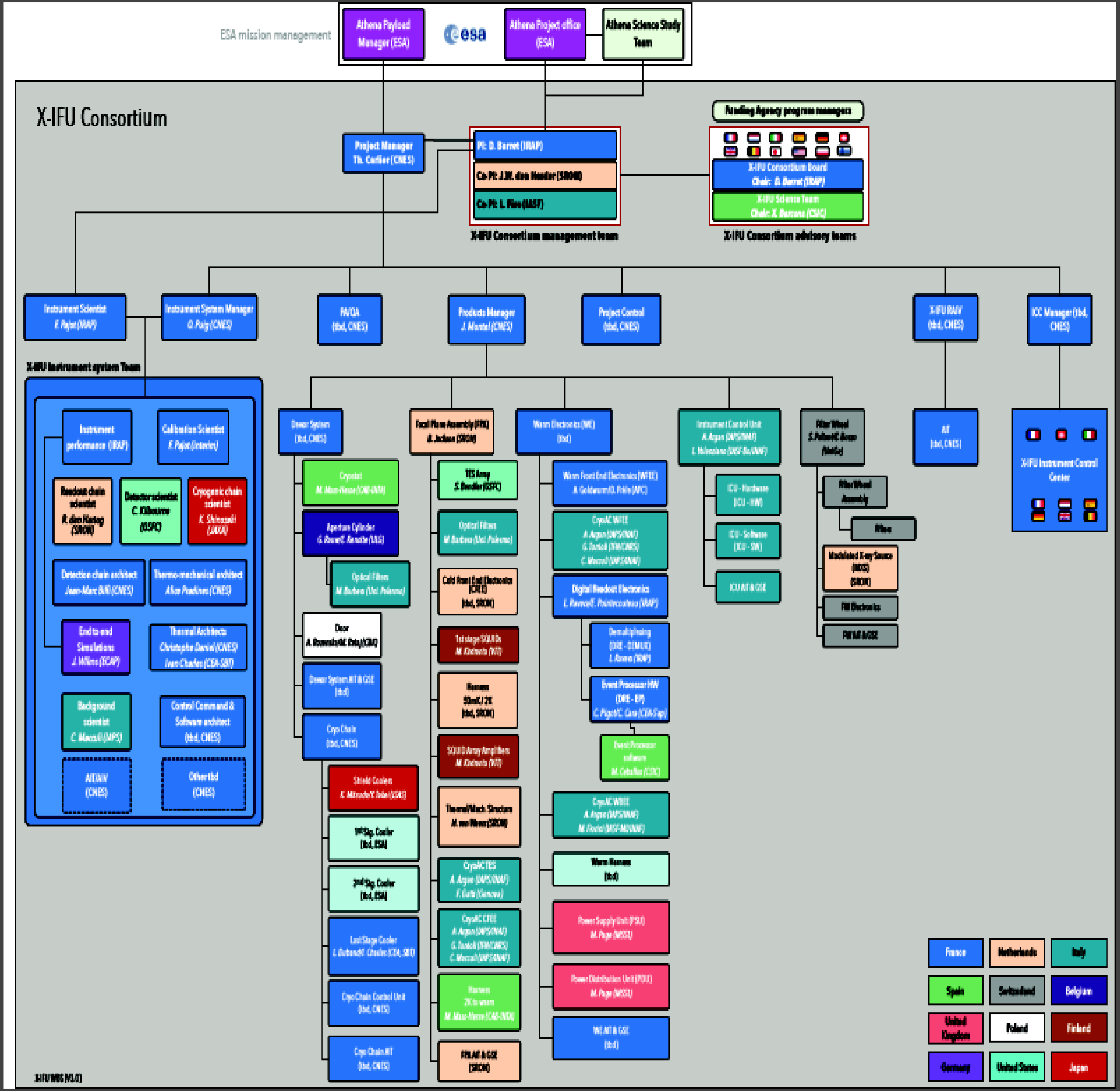

ESA mission management
Athena Payload Manager (ESA)
esa
Athena Project office (ESA)
Athena Science Study Team
X-IFU Consortium
Project Manager Th. Carlier (CNES)
PI: D. Barret (IRAP)
Co-PI: J.W. den Herder (SRON)
Co-PI: L. Piro (IAPS)
X-IFU Consortium management team
Funding Agency program managers
X-IFU Consortium Board Chair: D. Barret (IRAP)
X-IFU Science Team
X-IFU Consortium advisory teams
Instrument Scientist F. Pajot (IRAP)
Instrument System Manager
PA/QA (tbd, CNES)
Products Manager J. Mandel (CNES)
Project Control (tbd, CNES)
X-IFU RAIV (tbd, CNES)
ICC Manager (tbd, CNES)
X-IFU Instrument system Team
Instrument performance (IRAP)
Calibration Scientist
Readout chain scientist
Detector scientist
Cryogenic chain scientist
Detection chain architect
Thermo-mechanical architect
End to end Simulations
Thermal Architects
Background scientist
Control Command & Software architect (tbd, CNES)
AIT/AIV (CNES)
Other tbd (CNES)
Dewar System (tbd, CNES)
Focal Plane Assembly (FPA)
Warm Electronics (WE) (tbd)
Instrument Control Unit
Filter Wheel
AIT (tbd, CNES)
X-IFU Instrument Control Center
Cryostat
Aperture Cylinder
Optical Filters
Door
Dewar System AIT & GSE (tbd)
Cryo Chain (tbd, CNES)
Shield Coolers
1st Stg. Cooler (tbd, ESA)
2nd Stg. Cooler (tbd, ESA)
Last Stage Cooler
Cryo Chain Control Unit (tbd, CNES)
Cryo Chain AIT (tbd, CNES)
TES Array
Optical Filters
Cold Front End Electronics (CFEE)
1st stage SQUIDs
Harness
SQUID Array Amplifiers
Thermal/Mech. Structure
CryoAC TES
CryoAC CFEE
Harness
FPA AIT & GSE (SRON)
Warm Front End Electronics (WFEE)
CryoAC WFEE
Digital Readout Electronics
Demultiplexing (DRE - DEMUX)
Event Processor HW (DRE - EP)
Event Processor software
CryoAC WBEE
Warm Harness (tbd)
Power Supply Unit (PSU)
Power Distribution Unit (PDU)
WE AIT & GSE (tbd)
ICU - Hardware (ICU - HW)
ICU - Software (ICU - SW)
ICU AIT & GSE
Filter Wheel Assembly
Filters
Modulated X-ray Source (MXS) (SRON)
FW Electronics
FW AIT & GSE
France
Netherlands
Italy
Spain
Switzerland
Belgium
United Kingdom
Poland
Finland
Germany
United States
Japan